

Comparative Analysis of Mutant Tyrosine Kinase Chemical Rescue^{†,‡}Kathryn E. Muratore,^{§,||,⊥} Markus A. Seeliger,^{§,#} Zhihong Wang,^{||} Dina Fomina,[#] Johnathan Neiswinger,^{||} James J. Havranek,[○] David Baker,^{○,▽} John Kuriyan,^{#,▽} and Philip A. Cole^{*,||}*Department of Pharmacology and Molecular Sciences, Johns Hopkins University School of Medicine, Baltimore, Maryland 21205, Department of Molecular and Cell Biology, University of California, Berkeley, California 94720, and Department of Biochemistry, University of Washington, Seattle, Washington 98195**Received January 14, 2009; Revised Manuscript Received March 3, 2009*

ABSTRACT: Protein tyrosine kinases are critical cell signaling enzymes. These enzymes have a highly conserved Arg residue in their catalytic loop which is present two residues or four residues downstream from an absolutely conserved Asp catalytic base. Prior studies on protein tyrosine kinases Csk and Src revealed the potential for chemical rescue of catalytically deficient mutant kinases (Arg to Ala mutations) by small diamino compounds, particularly imidazole; however, the potency and efficiency of rescue was greater for Src. This current study further examines the structural and kinetic basis of rescue for mutant Src as compared to mutant Abl tyrosine kinase. An X-ray crystal structure of R388A Src revealed the surprising finding that a histidine residue of the N-terminus of a symmetry-related kinase inserts into the active site of the adjacent Src and mimics the hydrogen-bonding pattern seen in wild-type protein tyrosine kinases. Abl R367A shows potent and efficient rescue more comparable to Src, even though its catalytic loop is more like that of Csk. Various enzyme redesigns of the active sites indicate that the degree and specificity of rescue are somewhat flexible, but the overall properties of the enzymes and rescue agents play an overarching role. The newly discovered rescue agent 2-aminoimidazole is about as efficient as imidazole in rescuing R/A Src and Abl. Rate vs pH studies with these imidazole analogues suggest that the protonated imidazolium is the preferred form for chemical rescue, consistent with structural models. The efficient rescue seen with mutant Abl points to the potential of this approach to be used effectively to analyze Abl phosphorylation pathways in cells.

Protein tyrosine kinases (PTKs)¹ are key enzymes in cell signaling and play roles in a wide range of diseases including cancer (1, 2). Several PTKs, including Abl, are targeted clinically with therapeutic agents, and others are the subject of pharmaceutical development (3). As members of the protein kinase superfamily, PTKs share conserved sequences and folds (2), and yet they show distinct substrate selectivity (4, 5) and modes of regulation (6). Evidence suggests that the mechanism of PTK-catalyzed phosphoryl transfer is dissociative, in which the bond to the leaving group ADP is largely broken prior to tyrosine phenol attack on the γ -phosphorus of ATP (7). The alignment, orientation, and

spacing of the tyrosine and ATP substrates by key active site residues are believed to be crucial in facilitating catalysis based on structural (8), mutagenic (9), and kinetic (10) studies.

The catalytic loop sequence, DLAARN, is conserved throughout the vast majority of the 90 human PTKs but differs in the nine members of the Src family, which have the sequence DLRAAN (Figure 1A) (2). This relocation of the Arg from the D+4 position in most PTKs to the D+2 position in the Src family suggests an unusual functional plasticity. A crystal structure of an insulin receptor tyrosine kinase–bisubstrate analogue complex is believed to capture the active conformation of the enzyme and reveals the orientation of the active site residues (8). This structure shows that the side chain of the catalytic loop Asp makes a hydrogen bond to the tyrosine hydroxyl and likely serves as the catalytic base. The catalytic loop Arg side chain makes apparent hydrogen bonds to this Asp side chain, as well as the substrate phenol oxygen. This triangle of hydrogen bonds (Figure 1B) appears to provide a scaffold that aligns the reactants. It is assumed that the Src Arg residue, located in the noncanonical D+2 position, fulfills a similar role to that of the catalytic loop Arg in the D+4 position in non-Src PTKs.

Mutagenic analysis of the catalytic loop Arg has been performed previously on PTK Csk (11) and Src (12). Mutation of the D+4 Arg in PTK Csk to Ala (R318A Csk) resulted in a dramatic k_{cat} drop of 3000-fold with relatively

[†] This work was supported by National Institutes of Health Grant CA74305 (P.A.C.), the Johnson & Johnson Fellowship of Life Science Research (M.A.S.), and the Jane Coffin Childs Memorial Fund for Medical Research (J.J.H.).

[‡] The PDB code for the structure here is 3GEQ.

* To whom correspondence should be addressed. Tel: 410-614-8849. Fax: 410-614-7717. E-mail: pcole@jhmi.edu.

[§] These authors contributed equally to this work.

^{||} Johns Hopkins University School of Medicine.

[⊥] Current address: Department of Chemistry, American University, Washington, DC 20016.

[#] University of California, Berkeley.

[○] University of Washington.

[▽] Howard Hughes Medical Institute.

¹ Abbreviations: AblKD, human c-Abl kinase domain; D+2, PTK with active loop sequence DLRAAN; D+4, PTK with active loop sequence DLAARN; PP2, 4-amino-5-(4-chlorophenyl)-7-(*tert*-butyl)pyrazolo[3,4-*d*]pyrimidine; PTK, protein tyrosine kinase; SrcKD, chicken c-Src kinase domain.

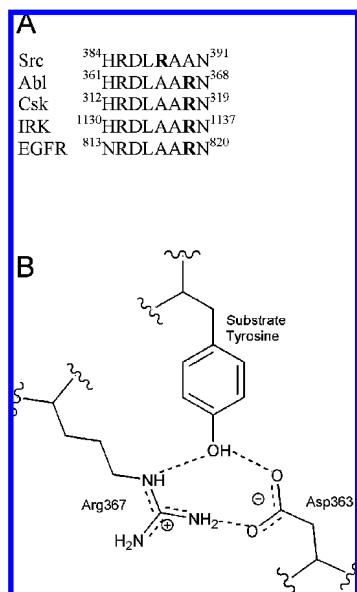


FIGURE 1: Catalytic loop of selected kinases. (A) Amino acid sequence of the catalytic loop region for Src (residues 384–391), Abl (residues 361–368), Csk, insulin receptor tyrosine kinase (IRK), and epidermal growth factor receptor kinase (EGFR). The D+2 Arg and D+4 Arg that are examined here are in bold. (B) Schematic of the interaction of the catalytic loop residues corresponding to Asp363 and Arg367 in Abl with the substrate tyrosine, as observed in the crystal structure of inhibited IRK.

small (<10-fold) K_m changes. A Csk double mutant was prepared to mimic the Src-like catalytic loop (D+2 Arg Csk), and this mutant showed a 150-fold increased kinase activity compared with R318A Csk (11). While still 20-fold less than wild type, the substantial kinase activity of the D+2 Arg Csk mutant bolsters the argument for functional plasticity of the catalytic loop Arg residue.

In some cases, enzyme active site point mutants can be chemically rescued by small molecules that complement the deleted side chains (13–15). Indeed, chemical rescue of R318A Csk with a series of diamino compounds (guanidiniums, amidiniums, imidazoles) could restore substantial activity to this mutant (11). Imidazole was the most efficient R318A Csk rescue agent, showed $K_m = 20$ mM, and stimulated kinase activity up to the level of the D+2 Arg Csk. Related studies were carried out on Src, and it was shown that mutation of the D+2 Arg in Src to Ala (R388A Src) is 200-fold less active than wild type (12). A Src double mutant that mimics the canonical catalytic loop (D+4 Arg Src) was 2-fold more active than wild type. Imidazole rescued R388A Src to a level of 50% of wild type, with a $K_m = 5$ mM.

The ability to rescue R318A Csk and R388A Src to 5–50% of wild-type k_{cat} values with a nontoxic concentration of imidazole (<50 mM) raised the interesting possibility that it might be feasible to complement these mutant tyrosine kinases in cells. Indeed, it was demonstrated that imidazole could restore Csk and Src functionality to mouse embryonic fibroblasts expressing replacement Arg → Ala mutant kinases (12, 16). Using this chemical rescue approach, new insights into the rapid signaling events have been obtained for Src and Csk (12, 17, 18).

Although progress on the chemical rescue of mutant Src and Csk has been made, questions remain. Does the imidazole occupy an active site position mimicking the

position of the catalytic loop Arg side chain? Are Arg → Ala mutant PTKs beyond Src and Csk likely to show more efficient chemical rescue, like Src, or less efficient rescue, like Csk? Can alternative potent rescue combinations of kinase mutations and small molecules be identified? Is the imidazole interacting with the mutant kinase as the imidazolium or the neutral species? Here we use a combination of X-ray crystallography and extended mutagenic and kinetic experiments on Abl and Src to address these questions.

EXPERIMENTAL PROCEDURES

Rosetta Design Calculations. The crystal structure of the insulin receptor tyrosine kinase (PDB code 1IR3) (19) was used as the scaffold for design calculations. Because the binding site for the small molecules used for chemical rescue was unknown, atoms comprising the guanidinium group of the mutated arginine residue (corresponding to R388 in chicken c-Src) were converted into a fixed ligand. Alternate amino acids were selected at positions corresponding to W428 and E454 in chicken c-Src. Side-chain conformational freedom was modeled with a backbone-dependent rotamer library (20) supplemented by extra sample points with χ_1 and χ_2 values ± 1 standard deviation in the observed torsional distributions. A Monte Carlo optimization algorithm was used to identify sequences and conformations that minimize the Rosetta full-atom energy potential of the complex (21).

Cloning, Expression, and Purification. Src and Abl variants were generated following QuikChange protocols, with the addition of 2% DMSO to the reaction mixture. The targeted mutagenesis was confirmed by DNA sequencing.

Src variants used in enzymatic assays were expressed as previously described (12). These preparations consisted of residues 85–533 of chicken c-Src. Double and triple mutants of R388A Src plus mutations at position 454 to alanine, lysine, or arginine and/or at position 428 to glutamate or glutamine resulted in very low expression levels and were not purified. Double mutants of R388A Src plus mutations at 428 to tyrosine, phenylalanine, and alanine were purified as previously described (12).

For the purposes of crystallization, the R388A mutant of the kinase domain of chicken c-Src (R388A SrcKD; residues 251–533) (22) was expressed and purified in *Escherichia coli* (23). R388A SrcKD was purified fused to an N-terminal TEV-cleavable His₆ tag, which results in a Gly-His-Met sequence before the start of the kinase domain sequence. The identity of the purified protein was confirmed by mass spectrometry (David King, Howard Hughes Medical Institute, Berkeley) and was found to be of the calculated mass without any posttranslational modification.

The previously described protocol for expression and purification of the Abl kinase domain (AblKD; residues 229–511 of human c-Abl) (23) was modified for the variants described here. By coexpressing AblKD with the catalytic domain of YopH phosphatase, instead of the full-length phosphatase, copurification of YopH and AblKD was mitigated. Therefore, only a single purification step with a Ni affinity column was performed. DTT (2 mM) was added to all purification steps, and the histidine tag was not cleaved prior to kinetic measurements.

The catalytic domain of YopH phosphatase (corresponding to residues 164–468) was subcloned with Pfu Turbo

polymerase and the primers 5'-AATTATCCATGGGCGGT-GAACGACCACA-3' and 5'-ACCCGCGGATCCTTAGC-TATTTAATAATGGTCGC-3'. pCDFDuet and the YopH PCR product were digested with *NcoI* and *BamHI* endonucleases. After dephosphorylation of digested pCDFDuet, both the vector and gene fragments were gel-purified (Qiaquick) and ligated together with T4 ligase. The final product was confirmed by DNA sequencing.

Synthesis of Biotin–Abltide. Abltide (EAIYAAPFAKKK) was synthesized using the Fmoc strategy on 0.2 mmol of Wang resin on a Rainin PS-3 peptide synthesizer. The DMF solvent was exchanged for NMP, and 60 mM biotin-oNP was allowed to couple overnight in the presence of 20 mM HOBT at room temperature on a rotator. A second 2 h coupling with 60 mM biotin-oNP and 20 mM HOBT was performed before cleavage of the peptide from the resin with 95% TFA and 2.5% triisopropylsilane. After ether precipitation, the crude peptide was purified by reverse-phase HPLC on a C₁₈ column. The peptide was eluted with a linear gradient (acetonitrile/water + 0.05% TFA) and lyophilized to dryness. Pure biotin–Abltide was dissolved in water and the pH adjusted to neutral with NaOH. The mass was confirmed by MALDI-TOF, and the concentration was determined by quantitative amino acid analysis at the Harvard Microchemistry and Proteomics Analysis Facility (Cambridge, MA).

Enzyme Kinetics. Three kinase assay methods were used to study the kinetics of the Src and Abl variants. All Src activity measurements were made using radiolabeled [γ -³²P]ATP and poly[Glu,Tyr] as the peptide substrate, with separation on SDS–PAGE as described previously (12). Phosphorylation of biotin–Abltide by Abl was detected spectrophotometrically as described in refs 24 and 25 or using radiolabeled ATP and selective binding to avidin following the method in ref 26. The coupling enzymes used in the spectrophotometric assay, pyruvate kinase and lactate dehydrogenase, were supplied by Sigma as ammonium sulfate suspensions.

Michaelis constants (K_m) and turnover numbers (k_{cat}) were determined by fixing the concentration of one substrate at $\geq 3 \times K_m$ and varying the concentration of the second substrate and fitting to eq 1.

$$v = \frac{k_{cat}[E][S]}{K_m + [S]} \quad (1)$$

Activators, such as imidazole, were treated as substrates, and activator-specific constants were derived from eq 1, as well.

Crystallization of R388A SrcKD. R388A SrcKD was crystallized using the hanging drop vapor diffusion method by mixing 1 μ L of protein at 6 mg/mL in 20 mM Tris, pH 8.0, 100 mM NaCl, 5% glycerol, 1 mM DTT, 50 mM imidazole, and 500 μ M PP2 (4-amino-5-(4-chlorophenyl)-7-(*tert*-butyl)pyrazolo[3,4-*d*]pyrimidine; Calbiochem) with 1 μ L of 50 mM imidazole, 500 μ M PP2, 20% PEG4000, 50 mM NH₄OAc, and 100 mM Bis-Tris, pH 5.5, over a 500 μ L reservoir of precipitant buffer. Rectangular crystals grew at room temperature within 8 h to 350 μ m \times 100 μ m \times 50 μ m. Crystals were cryoprotected in mother liquor plus 20% glycerol and flash frozen in liquid nitrogen.

Crystal Data Collection and Refinement. X-ray diffraction data were collected over 180° in 180 frames with 1°

Table 1: Data Collection and Refinement Statistics for R388A SrcKD Structure Determination

Data Collection	
beamline	ALS 8.3.1
resolution (Å)	50–2.2 (2.28–2.2) ^b
space group	P2 ₁
unit cell parameters	
<i>a</i> , <i>b</i> , <i>c</i> (Å)	59.65, 63.46, 83.86
$\alpha = \gamma$, β (deg)	90, 91.45
content of asymmetric unit	two kinase domains, two molecules of PP2
no. of measured reflections	110199
no. of unique reflections	31912
data redundancy	3.5
data completeness (%)	98.7 (93.9)
R_{sym} (%) ^a	9.4 (48.9)
I/σ	13.5 (2.3)
Refinement	
<i>R</i> factor/ <i>R</i> free (%)	22.6/27.3
no. of protein atoms	4356
no. of non-protein atoms	282
rmsd bond length (Å)	0.0076
rmsd bond angle (deg)	1.2
rmsd <i>B</i> factors (Å ²) (main chain/side chain)	1.5/2.1
PDB entry	3GEQ

^a $R_{sym} = \sum I - \langle I \rangle / \sum I$, where I is the observed intensity of a reflection and $\langle I \rangle$ is the average intensity of all the symmetry-related reflections. ^b Average (highest resolution shell).

oscillation at beamline 8.3.1 at the Advanced Light Source (ALS, Lawrence Berkeley National Laboratory). Reflections were indexed and merged in P2₁ with unit cell dimensions of $a = 59.65$ Å, $b = 63.46$ Å, $c = 83.86$ Å, $\alpha = 90^\circ$, $\beta = 91.45^\circ$, $\gamma = 90^\circ$ using DENZO, and data were scaled with Scalepack via the HKL2000 interface (27). The structure was solved by molecular replacement using the kinase domain of human c-Src of PDB entry 1Y57 (28) (residues 260–520) minus the C-helix (residues 298–310) and the activation loop (residues 400–425) as the template in Phaser (29) of ccp4i (30). The structure was built in O (31) and Coot (32), and refinement of the structure was straightforward in CNS (33).

RESULTS

Overall Structure of the Mutant Kinase Is Conserved. Protein kinases have been shown to yield crystals more easily and form better ordered crystals when complexed with ligands that bind to the kinase active site. Therefore, we decided to use the nonspecific Src kinase family inhibitor, PP2, which inhibits Src with nanomolar affinity, to improve crystallization. The protein crystallized readily in a variety of conditions: for some conditions within minutes of mixing the mother liquor with the protein solution. However, the fast crystallization yielded unusable groups of clustered crystals, and we screened further buffer conditions to control crystallization onset and growth speed (see Experimental Procedures). Data were recorded at ALS beamline 8.3.1 (Lawrence Berkeley National Laboratory) and crystals diffracted X-rays to 2.2 Å. The structure was solved by molecular replacement (Table 1 and Experimental Procedures) with two molecules of R388A SrcKD per asymmetric unit and each kinase in complex with one molecule of PP2.

The kinase domains show the canonical fold of the α/β -N-lobe and the α -helical C-terminal lobe (Figure 2) with the high-affinity ligand PP2 bound to the nucleotide binding

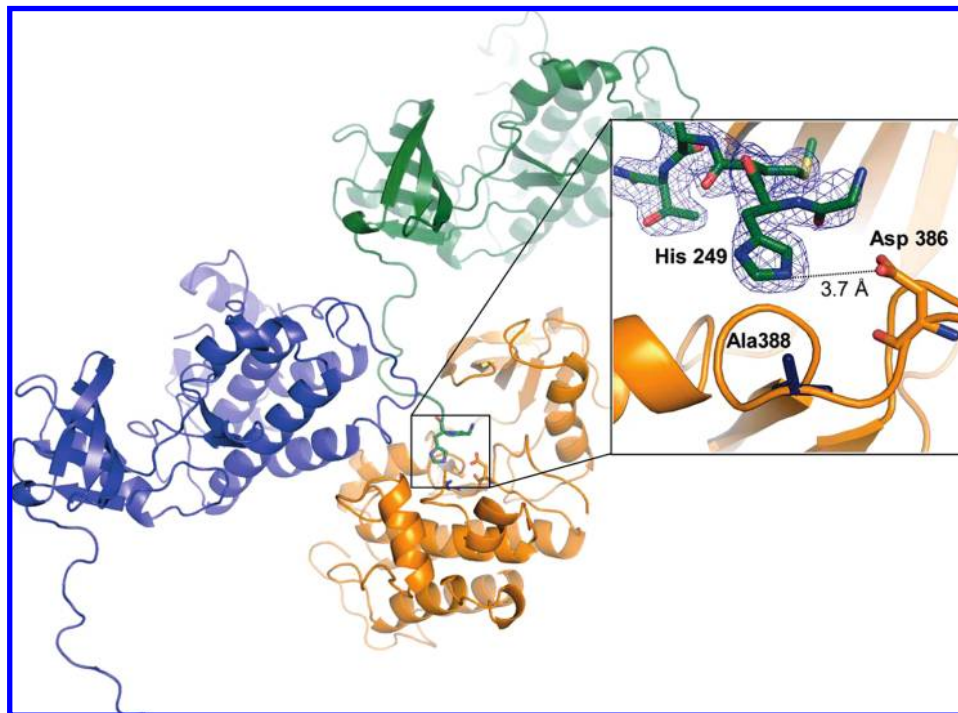


FIGURE 2: Extension of the N-terminus of one R388A SrcKD molecule into the active site of another. The relative orientation of three kinase molecules is shown as observed in the crystal. The N-terminal kinase domain–SH2 domain linker extends for 27 Å, inserting the side chain of His249 (green) deep into the active site of another molecule (orange), complementing the cavity created by the R388A mutation (pop-out).

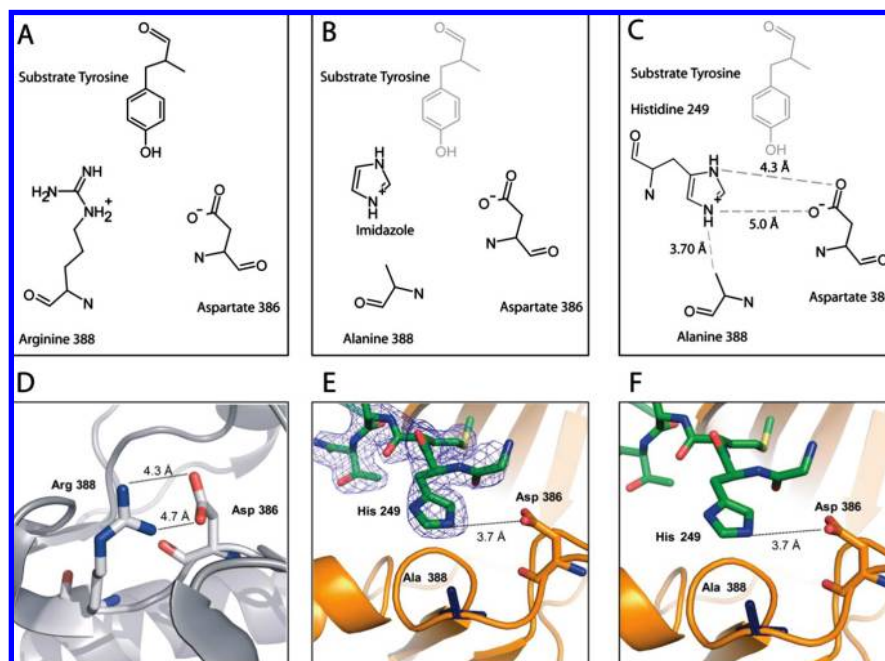


FIGURE 3: Occupation of histidine in the R388A SrcKD active site. (A) Orientation of the catalytic residues and substrate tyrosine in the structure of insulin receptor kinase (PDB entry 1IR3; Src numbering) (19). (B) Model for chemical rescue of R388A Src by imidazole as proposed by Qiao et al. (12). The protonated imidazolium fulfills the hydrogen-bonding network between the catalytic residues and the substrate tyrosine. (C) Schematic drawing of the coordination of His249 by the active site residues. (D) Distances between the active site residues of wild-type Src in the absence of substrate peptide (PDB entry 1Y57). (E, F) Structure of R388A SrcKD with electron density of the $2F_o - F_c$ contoured to 1σ . The His249 residue of a symmetry-related molecule (green) inserts into the active site of a kinase (orange). The distances for this structure are virtually identically to the distances in the wild-type Src structure, which is also free of substrate peptide.

pocket as seen before for Lck kinase (34). The two kinase domains in the asymmetric unit are virtually identical and align onto each other with a C_α rmsd of 0.241 Å. R388A SrcKD and the kinase domain of the molecular replacement

search template, human Src (PDB entry 1Y57), align with a C_α rmsd of 0.8 Å when the residues N-terminal of W260 are omitted from the rmsd calculation. The salt bridge between D310 of the C-helix and K295 is formed in R388A

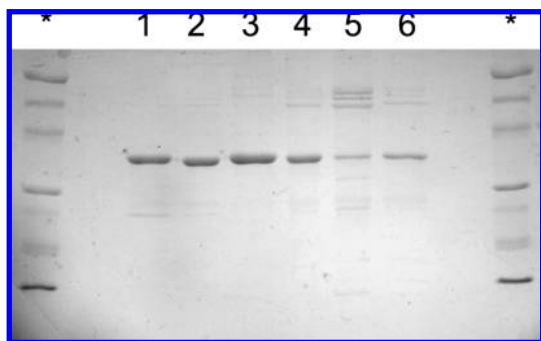


FIGURE 4: SDS-PAGE of purified AblKD enzyme variants. Molecular weight markers are indicated by asterisks. Numbered lanes are (1) wild-type AblKD, (2) R367A, (3) A365R + R367A, (4) R367A + W428Y, (5) R367G, and (6) A365G + R367A.

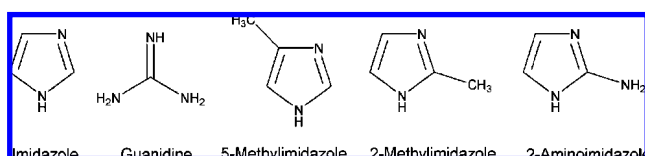


FIGURE 5: Diamino analogues. Structures of the chemical rescue agents used in this study.

SrcKD, which is the hallmark of the catalytically active kinase. The activation loop in R388A SrcKD is disordered between residues 412 and 424 as is often seen in tyrosine kinases without activation loop phosphorylation.

Structure of the Site of Mutation Shows Binding of the N-Terminal Histidine. Based on the model described previously for the chemical rescue of R388A Src (Figure 3B) (12), we expected to see electron density for imidazole in the vicinity of the side chain of residue 388 since it was present at 50 mM in the crystallization solution. Surprisingly, there was not only density to accommodate imidazole but a

continuous stretch of electron density extended from the expected imidazole binding site to the N-terminus of a symmetry-related molecule (Figures 3E and 2). We were able to build the N-terminus of the kinase up to the very first residue of the expressed and purified construct and found that the histidine side chain of the second residue in our construct occupies the expected position of the imidazole (Figure 3C). Whereas the N-terminal SH2-kinase domain linker in 1Y57 (residues 245–260) is bound to the SH3 domain, it is extended in the R388A SrcKD mutant (Figure 2). This is all the more surprising as the first two residues of our construct (Gly and His) are non-native; they are part of the TEV recognition sequence for the cleavable affinity tag.

We were surprised that the kinase domain would be able to accommodate the N-terminal peptide in a mode that has not been seen for substrate peptides before and which is almost certainly not physiological for a number of reasons: (1) the intruding N-terminus occludes the ATP binding site which is only partially occupied by PP2; (2) the kinase domain construct used in this study is preceded by bulky SH3 and SH2 domains in the full-length Src kinase; and (3) dynamic light scattering and size exclusion chromatography showed that R388A SrcKD is monomeric in solution at concentrations of up to 1 mg/ml, a concentration that almost certainly exceeds the cellular concentration of Src.

This cloning and crystallization artifact is very helpful in determining the binding mode of imidazole. The fact that histidine takes the position of the imidazole reduces the number of possible rotations of the imidazole ring from five for imidazole to two for the histidine (180° rotation around the C_α–C_β bond). We found that a favorable side-chain rotation of His 249 that fit the electron density yielded distances between the imidazolium nitrogens and the oxygen

Table 2: Kinetic Constants of Abl Variants^a

	[imidazole] (mM)	Abltide ^b			ATP ^c		
		k_{cat} (s ⁻¹)	K_m (μM)	k_{cat}/K_m (M ⁻¹ s ⁻¹)	k_{cat} (s ⁻¹)	K_m (μM)	k_{cat}/K_m (M ⁻¹ s ⁻¹)
wild-type AblKD	0	12 ± 1	60 ± 20	190000 ± 50000	9.9 ± 0.2	45 ± 3	220000 ± 20000
	40	12.7 ± 0.9	38 ± 9	330000 ± 80000	12.5 ± 0.2	41 ± 2	300000 ± 20000
R367A AblKD	0	NS (>0.04)	NS (>500)	35 ± 9			
	40	8.9 ± 0.3	130 ± 20	68000 ± 8000	5.6 ± 0.1	47 ± 5	120000 ± 10000
A365R/R367A AblKD	0	22 ± 1	280 ± 30	80000 ± 10000	13.2 ± 0.4	114 ± 9	115000 ± 9000

^a Reactions were performed at 30 °C in 100 mM Tris, pH 7.4, and 10 mM MgCl₂. NS: no saturation. If no value is given, then the constants were not measured. ^b For wild-type AblKD and R367A AblKD reactions without imidazole, [^γ-³²P]ATP = 0.15 mCi/mL and ATP = 0.25 mM ATP. For wild-type AblKD with imidazole, [^γ-³²P]ATP = 0.15 mCi/mL and ATP = 1 mM ATP. Otherwise, reaction mixtures contained 1 mM ATP, 0.1 unit/μL pyruvate kinase, 0.05 unit/μL lactate dehydrogenase, 1 mM phosphoenolpyruvate, 150 μM NADH, and 0.5 mM Na₃VO₄. ^c Reaction mixtures included 0.1 unit/μL pyruvate kinase, 0.05 unit/μL lactate dehydrogenase, 1 mM phosphoenolpyruvate, 150 μM NADH, and 0.5 mM Na₃VO₄. For wild-type AblKD, [Abltide] = 190 μM; for R367A AblKD, [Abltide] = 440 μM; for A365R/R367A AblKD, [Abltide] = 840 μM.

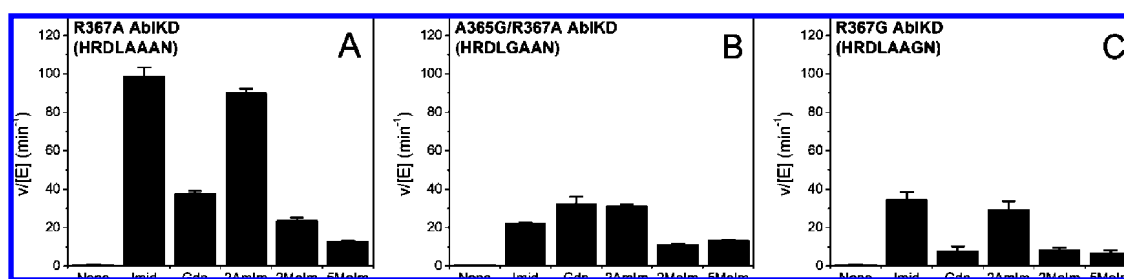


FIGURE 6: Rescue of AblKD variants with diamino analogues. Relative activation of AblKD variants by imidazole (Imid), guanidine (Gdn), 2-methylimidazole (2MeIm), or 5-methylimidazole (5MeIm) compared to basal activity (none). The letters in parentheses indicate the catalytic loop sequence. Activity was measured at 30 °C using 40 mM indicated activator in 100 mM Tris, pH 7.4, 10 mM MgCl₂, 500 μM ATP, 2 mM Abltide, and 0.15 mCi/mL [^γ-³²P]ATP.

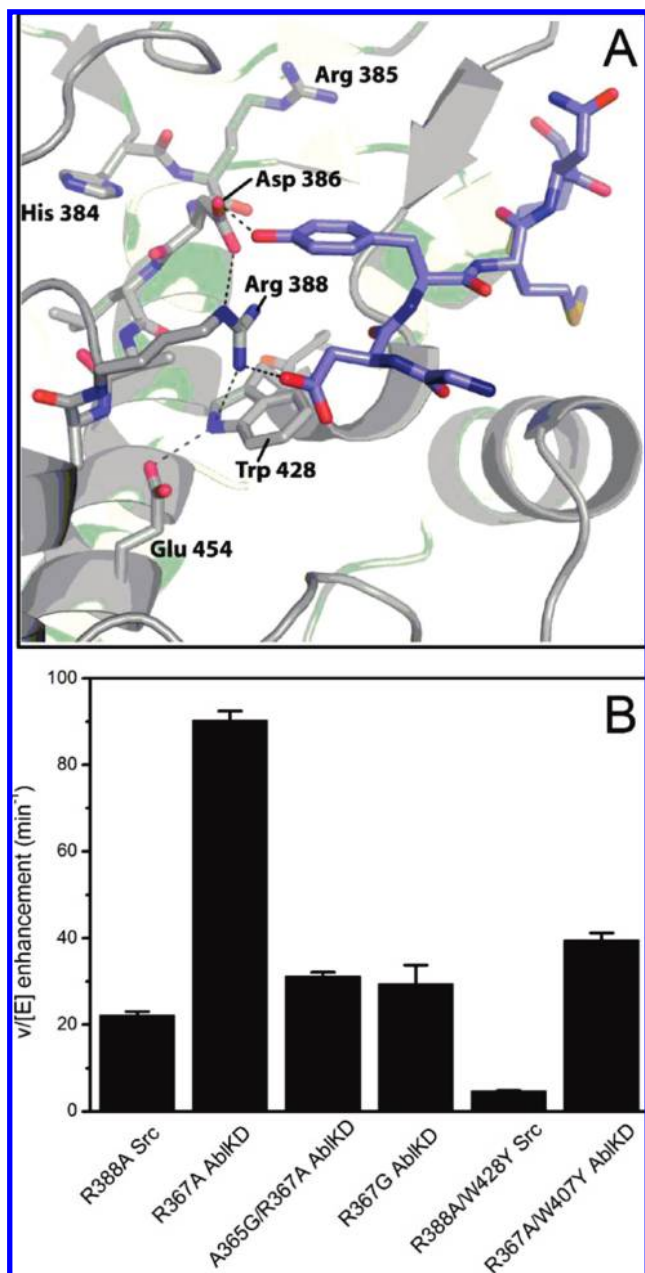


FIGURE 7: Modulation of chemical rescue. (A) Interactions of Trp428 and Glu454 (Src numbering) as seen in the crystal structure for IRK (PDB entry 1IR3). Peptide inhibitor is shown in blue, while the kinase backbone is shown in gray. Stick representations are used for side chains of the active site loop (HRDLAAR) as well as the conserved tryptophan and glutamate. Hydrogen-bonding interactions are shown as dashed lines. (B) Relative activation of AblKD and Src variants by 2-aminoimidazole compared to no activator. Note that, due to the different substrate preferences, AblKD activity is significantly higher than Src activity. Trp407 in Abl corresponds to Trp428 in Src. Src activity was measured as in Table 2 using 50 mM 2-aminoimidazole; Abl assays are as described for Figure 6 (using 40 mM 2-aminoimidazole).

atoms of the catalytic aspartate side chain D386 comparable to R388–D386 distances in wild-type Src structures (Figure 3). Note that these distances are longer than those in the IRK ternary complex and presumably tighten up when peptide substrate binds. In any case, this structure implicitly suggests a natural affinity for the imidazole in the R388A mutant of Src.

Investigation of the Catalytic Loop Arg367 Residue in Abl. Generation of wild-type and mutant Abl kinase domains was

performed using a modified *E. coli* expression system which overcomes host toxicity by coexpressing a tyrosine phosphatase (YopH) (23). One technical improvement over the original method was to use a truncated YopH construct that shows reduced affinity to Ni resin and is therefore more readily separated during this purification step. Purity of Abl kinase mutants is shown in Figure 4.

Kinetic analyses of wild-type Abl and Abl mutants were performed with an efficient Abl peptide substrate (Abltide, biotin–EAIYAAPFAKKK) and a direct, [³²P]ATP incorporation quenched assay (26) as well as a continuous (spectrophotometric) coupled assay (25). Both assay methods gave similar catalytic parameters. As shown in Table 2, the mutation of the D+4 Arg to Ala (R367A AblKD) showed a reduction in catalytic efficiency ($k_{\text{cat}}/K_m = 35 \text{ M}^{-1} \text{ s}^{-1}$) of about 5000-fold compared with the wild-type enzyme ($k_{\text{cat}}/K_m = 1.9 \times 10^5 \text{ M}^{-1} \text{ s}^{-1}$). Given the slow kinase rate of R367A AblKD, it was not possible to accurately determine the K_m values for this mutant. Interestingly, the R367A/A365R AblKD double mutant showed a k_{cat}/K_m ($80000 \text{ M}^{-1} \text{ s}^{-1}$) value within 2-fold of wild-type AblKD, suggesting excellent compensation by moving the Arg to the D+2 position seen in Src.

The catalytic rescue of R367A AblKD was examined with a series of diamino analogues that have been tested previously with Csk (11) and Src (12) including guanidinium, imidazole, 2-methylimidazole, and 5-methylimidazole (Figure 5). All showed the ability to stimulate R367A AblKD at least 5-fold, but maximal stimulation was achieved with imidazole (100-fold; Figure 6A). More extensive analysis of imidazole rescue of R367A AblKD revealed that it could afford k_{cat}/K_m ($68000 \text{ M}^{-1} \text{ s}^{-1}$) within 3-fold of the wild-type level (Table 2), with minor changes in k_{cat} and K_m . Imidazole had minimal impact on the wild-type AblKD kinase parameters, as shown in Table 2. The K_m of imidazole is 8.5 mM, similar to the K_m for rescue of R388A Src (5 mM) (12). We also examined the rescue of two other Abl mutants that were analogous to those studied previously in Src, R367G AblKD and R367A/A365G AblKD, which have the potential to expand the cavity surrounding the deleted Arg side chain. These mutants were also quite catalytically impaired compared to wild type, as expected, and complementation by imidazole was less efficient (Figure 6B,C). It is noteworthy that the methylimidazoles showed a similar efficacy (within 3-fold) for R367A/A365G AblKD, suggesting that the larger hole could be filled more effectively by the larger imidazole analogue. Related behavior was observed with Src rescue (12). Taken together, the Abl chemical rescue data are quantitatively more similar to those of Src than Csk.

Second Sphere Mutation and Aminoimidazole Complementation in Src and Abl. We investigated the interactions of kinase residues that might influence chemical rescue efficiency and small molecule selectivity. A computational analysis using Rosetta (21) was undertaken to select “second-sphere” residues that might be most important. The mutations that were selected fell into two types: (1) mutations that filled in the space vacated by the Arg → Ala mutation and (2) substitutions of different interactions for the Glu454–Tyr428 hydrogen bond. We pursued these studies on the well-characterized Src enzyme initially. The mutants made to address the former case were not activatable by imidazole (data not shown). This may be due to uncertainty in the

Table 3: Comparison of Imidazole and 2-Aminoimidazole as Activators^a

	imidazole			2-aminoimidazole		
	k_{cat} (min^{-1})	K_m (mM)	k_{cat}/K_m ($\text{M}^{-1} \text{s}^{-1}$)	k_{cat} (min^{-1})	K_m (mM)	k_{cat}/K_m ($\text{M}^{-1} \text{s}^{-1}$)
R388A Src ^b	21.5 ± 0.7	9.3 ± 0.8	40 ± 10	11.0 ± 0.3	6.8 ± 0.5	27 ± 2
R388A/W428Y Src ^b	8.30 ± 0.02	16 ± 1	8.7 ± 0.8	5.56 ± 0.03	6 ± 1	16 ± 3
R367A AblKD ^c	460 ± 20	8.5 ± 0.9	900 ± 100	350 ± 20	5.3 ± 0.9	1100 ± 200
R367A/W407Y AblKD ^d	NS (>60)	NS (>30)	26 ± 7			

^a Reactions were performed at 30 °C at pH 7.4 with 10 mM MgCl₂. NS: no saturation. If no value is given, then the constants were not measured. ^b 50 mM Tris, 10 mM DTT, 200 μg/mL BSA, 400 μM ATP, 1 mg/mL PGT, and 0.15 mCi/mL [γ -³²P]ATP. ^c 100 mM Tris, 1 mM ATP, 440 μM Abltide, 0.1 unit/μL pyruvate kinase, 0.05 unit/μL lactate dehydrogenase, 1 mM phosphoenolpyruvate, 150 μM NADH, and 0.5 mM Na₃VO₄. ^d 100 mM Tris, 1 mM ATP, 1.5 mM Abltide, 0.1 unit/μL pyruvate kinase, 0.05 unit/μL lactate dehydrogenase, 1 mM phosphoenolpyruvate, 150 μM NADH, and 0.5 mM Na₃VO₄.

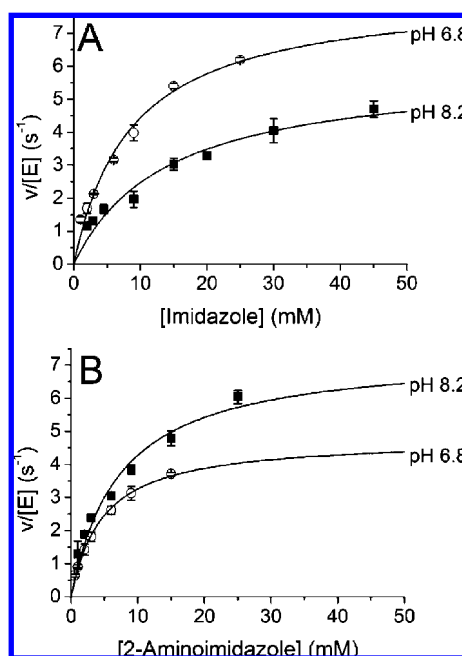


FIGURE 8: Effect of pH on rescue of Abl R367A by imidazole and 2-aminoimidazole. (A) Activation by imidazole ($pK_a = 7.0$) and (B) 2-aminoimidazole ($pK_a = 8.5$) of R367A AblKD at pH 6.8 and 8.2 was fit to eq 1. Reactions were performed at 30 °C in 100 mM HEPES, 10 mM MgCl₂, 1 mM ATP, 440 μM Abltide, 0.1 unit/μL pyruvate kinase, 0.05 unit/μL lactate dehydrogenase, 1 mM phosphoenolpyruvate, 150 μM NADH, and 0.5 mM Na₃VO₄ at the indicated pH.

placement of the guanidinium ligand, and the additional atoms in the mutant side chain may occlude the ligand binding site. For the second class of mutations selected by Rosetta, Trp428 and Glu454 were replaced by a series of amino acids. These mutations were carried out in a background of R388A. In Figure 7A, we highlight the observed interactions of Trp428 and Glu454 with active site residues. Many of the double (and triple) mutants expressed poorly in *E. coli* or appeared to be very unstable in kinase assays, making characterization very difficult. These problems may indicate the importance of a cation- π interaction between the guanidinium/imidazolium and the residue at that position.

One mutant, R388A/W428Y Src, showed sufficient stability and baseline kinase activity to determine the kinetic parameters. It showed modestly less efficient rescue (4.6-fold) than the parent R388A Src itself. We also assessed this and other mutants with an additional, novel rescue agent, 2-aminoimidazole, which in the course of this work was found to efficiently rescue R388A Src and R367A AblKD (about 30–40% more potent than imidazole in terms of K_m). As shown in Table 3, 2-aminoimidazole was about equally

effective (within 2-fold) at rescuing R388A/W428Y Src as the parent R388A Src, suggesting a relative compensation compared to imidazole. These findings support the idea that Trp428 can subtly influence the preference for rescue agent. However, the results with Abl were quite different. R367A/W407Y AblKD was greatly catalytically impaired and was only poorly rescueable by imidazole (35-fold down in k_{cat}/K_m compared to parent R367A AblKD). Despite the generally conserved chemical rescue properties of Abl and Src, Trp407 in Abl appears to be more crucial to facilitating imidazole rescue than the corresponding Trp428 residue in Src.

Analysis of the Imidazole Protonation State in Chemical Rescue. More extensive analysis of Src and Abl mutants (Figures 6 and 7) revealed similar trends for chemical rescue by imidazole and 2-aminoimidazole, suggesting that the general interactions of these compounds with these PTKs are similar. Because imidazole has $pK_a = 7.0$ and 2-aminoimidazole has $pK_a = 8.5$ (35), we hypothesized that an analysis of the pH effects of chemical rescue by these compounds might provide information about the protonation state of the analogue employed for chemical rescue. As shown in Figure 8, imidazole effects greater rescue of R367A AblKD than 2-aminoimidazole when both are studied at pH 6.8 and each is >50% protonated. In contrast, chemical rescue by 2-aminoimidazole is superior to imidazole at pH 8.2, when only the 2-aminoimidazole is greater than 50% protonated. These data are consistent with the model that the imidazolium is a more potent rescue agent than the neutral imidazole form of these compounds.

DISCUSSION

Kinetic experiments done on Csk, Src, and now Abl, in which complementation of various single and double Arg mutant PTKs by several compounds (guanidinium, imidazole, methylimidazoles), argue for localization of the rescue agent in the mutant cavity. The surprising findings from X-ray crystallography of R388A SrcKD provides independent evidence that chemical rescue of mutant PTKs involves the positioning of an imidazole in place of the native Arg. Electron density for a His residue from one kinase molecule in the active site of a second was unexpected for two reasons. First, Src is a monomer in solution so that preexisting dimeric interactions were not known. Second, it has been shown previously that the catalytic loop Arg \rightarrow His mutant of Csk is about as dead as the Arg \rightarrow Ala mutant, and free His in solution is a rather poor rescue agent compared with imidazole (11). We can rationalize the inactivity of the Arg \rightarrow His Csk mutant as due to inability of His to extend far enough into the active site. The fact that free His is a poor

rescue agent could be due to the added bulk of the alanyl moiety of the residue, creating unfavorable interactions. Additionally, in the R388A SrcKD crystal structure, the backbone atoms of His seem to prevent effective ATP binding; thus free His may have the same effect and serve to inactivate the kinase. For these reasons, rescue of AblKD variants with free His was not attempted.

The relatively high efficiency of R387A AblKD chemical rescue bodes well for future applications in cell signaling studies. Abl rescue efficiency is more similar to Src's than Csk's. This is significant because Abl's catalytic loop sequence is identical to that of Csk and different from that of Src. This suggests that residues outside the catalytic loop are more influential in governing rescue efficiency. However, Csk is, in many ways, an outlier PTK because of its high substrate selectivity for one Tyr site in the Src protein and low rate of phosphorylation of peptides (36). Recent studies on Csk's naturally truncated activation loop suggest that its unique activation loop may contribute to its unique properties (37).

The discovery of 2-aminoimidazole as a new and potent rescue agent for mutant PTKs may have practical importance for cell signaling studies. Its structure can be viewed as a hybrid molecule of guanidinium and imidazole, perhaps accounting for its improved properties over 2-methylimidazole. In this study, it provided a useful tool for establishing the preference for the imidazolium form of the rescue agent to complement mutant Src and Abl. This protonation state is consistent with expectation since the Arg pK_a is above 10 and likely to be protonated in the active site. Furthermore, the enhanced electrostatic interaction of the catalytic base Asp carboxylate with the imidazolium is likely to be catalytically important in substrate alignment.

ACKNOWLEDGMENT

We thank Steve Zimmerman and members of the Cole laboratory for helpful ideas and discussions. Crystallographic data were collected at the Advanced Light Source, supported by the Director, Office of Science, Office of Basic Energy Sciences, of the U.S. Department of Energy under Contract DE-AC02-05CH11231.

REFERENCES

- Blume-Jensen, P., and Hunter, T. (2001) Oncogenic kinase signalling. *Nature* 411, 355–365.
- Manning, G., Plowman, G. D., Hunter, T., and Sudarsanam, S. (2002) Evolution of protein kinase signaling from yeast to man. *Trends Biochem. Sci.* 27, 514–520.
- Krause, D. S., and Van Etten, R. A. (2005) Tyrosine kinases as targets for cancer therapy. *N. Engl. J. Med.* 353, 172–187.
- Miller, W. T. (2003) Determinants of substrate recognition in nonreceptor tyrosine kinases. *Acc. Chem. Res.* 36, 393–400.
- Songyang, Z., Carraway, K. L., III, Eck, M. J., Harrison, S. C., Feldman, R. A., Mohammadi, M., Schlessinger, J., Hubbard, S. R., Smith, D. P., Eng, C., et al. (1995) Catalytic specificity of protein-tyrosine kinases is critical for selective signalling. *Nature* 373, 536–539.
- Huse, M., and Kuriyan, J. (2002) The conformational plasticity of protein kinases. *Cell* 109, 275–282.
- Parang, K., and Cole, P. A. (2002) Designing bisubstrate analog inhibitors for protein kinases. *Pharmacol. Ther.* 93, 145–157.
- Parang, K., Till, J. H., Ablooglu, A. J., Kohanski, R. A., Hubbard, S. R., and Cole, P. A. (2001) Mechanism-based design of a protein kinase inhibitor. *Nat. Struct. Biol.* 8, 37–41.
- Williams, D. M., and Cole, P. A. (2002) Proton demand inversion in a mutant protein tyrosine kinase reaction. *J. Am. Chem. Soc.* 124, 5956–5957.
- Kim, K., and Cole, P. A. (1998) Kinetic analysis of a protein tyrosine kinase reaction transition state in the forward and reverse directions. *J. Am. Chem. Soc.* 120, 6851–6858.
- Williams, D. M., Wang, D., and Cole, P. A. (2000) Chemical rescue of a mutant protein-tyrosine kinase. *J. Biol. Chem.* 275, 38127–38130.
- Qiao, Y., Molina, H., Pandey, A., Zhang, J., and Cole, P. A. (2006) Chemical rescue of a mutant enzyme in living cells. *Science* 311, 1293–1297.
- Toney, M. D., and Kirsch, J. F. (1989) Direct Bronsted analysis of the restoration of activity to a mutant enzyme by exogenous amines. *Science* 243, 1485–1488.
- Craik, C. S., Rocznik, S., Largman, C., and Rutter, W. J. (1987) The catalytic role of the active site aspartic acid in serine proteases. *Science* 237, 909–913.
- Tu, C. K., Silverman, D. N., Forsman, C., Jonsson, B. H., and Lindskog, S. (1989) Role of histidine 64 in the catalytic mechanism of human carbonic anhydrase II studied with a site-specific mutant. *Biochemistry* 28, 7913–7918.
- Lowry, W. E., Huang, J., Ma, Y. C., Ali, S., Wang, D., Williams, D. M., Okada, M., Cole, P. A., and Huang, X. Y. (2002) Csk, a critical link of g protein signals to actin cytoskeletal reorganization. *Dev. Cell* 2, 733–744.
- Madhusoodanan, K. S., Guo, D., McGarrigle, D. K., Maack, T., and Huang, X. Y. (2006) Csk mediates G-protein-coupled lysophosphatidic acid receptor-induced inhibition of membrane-bound guanylyl cyclase activity. *Biochemistry* 45, 3396–3403.
- Im, E., and Kazlauskas, A. (2007) Src family kinases promote vessel stability by antagonizing the Rho/ROCK pathway. *J. Biol. Chem.* 282, 29122–29129.
- Hubbard, S. R. (1997) Crystal structure of the activated insulin receptor tyrosine kinase in complex with peptide substrate and ATP analog. *EMBO J.* 16, 5572–5581.
- Dunbrack, R. L., Jr., and Cohen, F. E. (1997) Bayesian statistical analysis of protein side-chain rotamer preferences. *Protein Sci.* 6, 1661–1681.
- Das, R., and Baker, D. (2008) Macromolecular modeling with rosetta. *Annu. Rev. Biochem.* 77, 363–382.
- Takeya, T., and Hanafusa, H. (1983) Structure and sequence of the cellular gene homologous to the RSV src gene and the mechanism for generating the transforming virus. *Cell* 32, 881–890.
- Seeliger, M. A., Young, M., Henderson, M. N., Pellicena, P., King, D. S., Falick, A. M., and Kuriyan, J. (2005) High yield bacterial expression of active c-Abl and c-Src tyrosine kinases. *Protein Sci.* 14, 3135–3139.
- Cook, P. F., Neville, M. E., Jr., Vrana, K. E., Hartl, F. T., and Roskoski, R., Jr. (1982) Adenosine cyclic 3',5'-monophosphate dependent protein kinase: kinetic mechanism for the bovine skeletal muscle catalytic subunit. *Biochemistry* 21, 5794–5799.
- Barker, S. C., Kassel, D. B., Weigl, D., Huang, X., Luther, M. A., and Knight, W. B. (1995) Characterization of pp60c-src tyrosine kinase activities using a continuous assay: autoactivation of the enzyme is an intermolecular autophosphorylation process. *Biochemistry* 34, 14843–14851.
- Qiu, C., Tarrant, M. K., Choi, S. H., Sathyamurthy, A., Bose, R., Banjade, S., Pal, A., Bornmann, W. G., Lemmon, M. A., Cole, P. A., and Leahy, D. J. (2008) Mechanism of activation and inhibition of the HER4/ErbB4 kinase. *Structure* 16, 460–467.
- Otwinowski, Z., and Minor, W. (1997) Processing of X-ray diffraction data collected in oscillation mode. *Macromol. Crystallogr., Part A* 276, 307–326.
- Cowan-Jacob, S. W., Fendrich, G., Manley, P. W., Jahnke, W., Fabbro, D., Liebetanz, J., and Meyer, T. (2005) The crystal structure of a c-Src complex in an active conformation suggests possible steps in c-Src activation. *Structure* 13, 861–871.
- McCoy, A. J., Grosse-Kunstleve, R. W., Storoni, L. C., and Read, R. J. (2005) Likelihood-enhanced fast translation functions. *Acta Crystallogr., Sect. D: Biol. Crystallogr.* 61, 458–464.
- Collaborative (1994) The CCP4 suite: programs for protein crystallography. *Acta Crystallogr., Sect. D* 50, 760–763.
- Jones, T. A., Zou, J. Y., Cowan, S. W., and Kjeldgaard, M. (1991) Improved methods for building protein models in electron-density maps and the location of errors in these models. *Acta Crystallogr., Sect. A* 47, 110–119.
- Krissinel, E., and Henrick, K. (2004) Secondary-structure matching (SSM), a new tool for fast protein structure alignment in three dimensions. *Acta Crystallogr., Sect. D: Biol. Crystallogr.* 60, 2256–2268.

33. Brunger, A. T., Adams, P. D., Clore, G. M., DeLano, W. L., Gros, P., Grosse-Kunstleve, R. W., Jiang, J. S., Kuszewski, J., Nilges, M., Pannu, N. S., Read, R. J., Rice, L. M., Simonson, T., and Warren, G. L. (1998) Crystallography & NMR system: A new software suite for macromolecular structure determination. *Acta Crystallogr., Sect. D: Biol. Crystallogr.* 54, 905–921.
34. Zhu, X., Kim, J. L., Newcomb, J. R., Rose, P. E., Stover, D. R., Toledo, L. M., Zhao, H., and Morgenstern, K. A. (1999) Structural analysis of the lymphocyte-specific kinase Lck in complex with non-selective and Src family selective kinase inhibitors. *Structure* 7, 651–661.
35. Storey, B. T., Sullivan, W. W., and Moyer, C. L. (1964) The pK_a values of some 2-aminimidazolium ions. *J. Org. Chem.* 29, 3118–3120.
36. Sondhi, D., Xu, W., Songyang, Z., Eck, M. J., and Cole, P. A. (1998) Peptide and protein phosphorylation by protein tyrosine kinase Csk: insights into specificity and mechanism. *Biochemistry* 37, 165–172.
37. Levinson, N. M., Seeliger, M. A., Cole, P. A., and Kuriyan, J. (2008) Structural basis for the recognition of c-Src by its inactivator Csk. *Cell* 134, 124–134.

BI900057G